Journal of Microscopy and Ultrastructure 2 (2014) 236–244

Contents lists available at ScienceDirect

Journal of Microscopy and Ultrastructure

journal homepage: www.elsevier.com/locate/jmau

Original Article

The effect of aging on impact toughness and fracture surface fractal dimension in SAF 2507 super duplex stainless steel

Oswaldo Hilders[a,*], Naddord Zambrano[b]

[a] Department of Physical Metallurgy, School of Metallurgical Engineering and Materials Science, Central University of Venezuela, Apartado 47514, Caracas 1041-A, Venezuela
[b] Foundation for Professional Development of the Venezuelan College of Engineering, Caracas 1050, Venezuela

ARTICLE INFO

Article history:
Received 28 April 2014
Received in revised form 28 June 2014
Accepted 6 July 2014
Available online 22 July 2014

Keywords:
Super duplex stainless steels
Fractography
Fracture toughness
Fractal dimension

ABSTRACT

The relation between room temperature impact toughness and fractal behavior of the fracture surfaces of SAF 2507 super duplex stainless steel, aged between 0 and 288 h at 475 °C, has been studied. Fractography was performed in a scanning electron microscope and the fractal dimension was determined according to the slit island method. A monotonical decrease in fractal dimension was observed as the time of aging increases from 0 to 288 h. For the entire range of aging times, a complete transition from ductile to brittle behavior was observed as the impact toughness decreases from 284 J (0-24 h) to 43 J (288 h). Ductile fracture occurred by nucleation growth and coalescence of micro-dimples, while the brittle behavior was characterized by the propagation of cleavage cracks in ferrite, controlled by plasticity of the surrounding austenite. Partially based on several previous concepts and relationships well established for brittle materials, a direct linear correlation between impact toughness and fractal dimensional increment has been developed. The concept of critical volume of material is proposed and tentatively related with the unstable crack propagation event, through both, the so called critical length (microstructurally significant distance) and the size of the largest micro-dimple and cleavage facet (structural parameter) developed in ductile and brittle fracture respectively.

1. Introduction

An attractive combination of mechanical properties and corrosion resistance is offered by SAF 2507 type (UNS S32750) super duplex stainless steel (SDSS), which has resulted in its extensive use by the offshore oil and gas industries [1,2]. Room temperature impact fracture toughness in this alloy is very high in the solution annealing condition [3], but several secondary phases impair its behavior [4–6]. One of these phases is the chromium-enriched alpha prime phase (α') which is expected to form at temperatures below 500 °C, and has been commonly studied at 475 °C [7–9]. Being SAF 2507 one of the most widely used SDSS grades, it is desirable to understand its impact toughness behavior from the point of view of the changes of the fracture morphology. Since the local stress state and fracture strain are different for different types of fracture morphologies in the same material, fractal geometry can be used to describe these morphologies, being useful not just as another quantitative fractographic method, but as a powerful tool for a better understanding of the different mechanisms of fracture [10–12]. Fractal dimension D, which is a quantitative descriptor of overall fracture surface, provides significant information on the surface topography and the processes responsible for its changes [13,14]. The objective of this work is to study

* Corresponding author. Tel.: +58 212 3725230; fax: +58 212 3725230.
E-mail address: ohilders@hotmail.com (O. Hilders).

http://dx.doi.org/10.1016/j.jmau.2014.07.001
2213-879X/

Table 1
Chemical composition of 2507 SDSS (weight %).

Cr	Ni	Mo	Mn	Si	P	S	N	C	Fe
22	4.5	2.5	2.0	1.0	0.03	0.02	0.10	0.03	bal

the relationship between the room temperature impact toughness of SAF 2507 SDSS and the fractal behavior of the corresponding fracture surfaces, after different aging treatments at 475 °C.

2. Material and methods

The SDSS used in this study was type 2507 supplied by AB Sandvik Steel® with the composition listed in Table 1. This material was fabricated into hot-rolled bars with diameter of 25.4 mm. Fig. 1 shows the two-phase microstructure of austenite islands (γ) elongated in the rolling direction and a ferrite matrix (α) in a proportion of ≈50/50. The microstructure was revealed by mechanical etching in $HCl + K_2S_2O_5$ solution. 40 standard Charpy v-notch impact specimens were prepared and solution-treated at 1100 °C for 30 min. After solution treatment, the specimens were water quenched, and 35 samples out of 40 were isothermally aged at 475 °C for 3, 9, 24, 72, 120, 192 and 288 h (5 samples for each time of treatment). The remaining 5 solution-treated samples will, subsequently, be referred to as "0 h" aged samples. All impact specimens were tested at room temperature in a universal impact test machine. Fractography of the broken samples was performed in a scanning electron microscope (SEM). The fracture surfaces were analyzed according to the slit island method (SIM) [15–17]. One fracture surface for each experimental condition was mounted in resin, and after a series of polishing operations parallel to the mean plane of fracture, a pattern of metallic "islands" was revealed. When the area A and the perimeter P are measured for a set of "islands" using the same ruler length, the fractal dimension D was obtained from full logarithmic scale diagrams of $\sum Pi$ vs. $\sum Ai$, being Pi and Ai the perimeter and the area of the ith island on a particular jth layer containing n such islands respectively. From the resulted straight curves the fractal dimension becomes: $D = 2 \times$ slope. Since D^* is the fractional part of the fractal dimension ($0 \le D^* \le 1$) it follows that

$$D^* = 2\left\{\frac{d\left[\log \sum_{i=1}^{n}(Pi)\right]}{d\left[\log \sum_{i=1}^{n}(Ai)\right]}\right\} - 1 \quad (1)$$

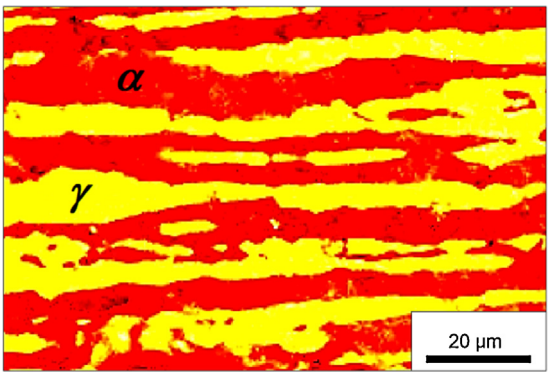

Fig. 1. Optical micrograph of the as-received microstructure of SAF 2507 SDSS (longitudinal section of the original hot-rolled bar).

3. Results and discussion

3.1. Fractography

3.1.1. Samples aged between 0 and 24 h

The fracture surfaces of the impact samples aged between 0 and 24 h are shown in Fig. 2. The intrinsic micromechanism governing fracture was nucleation growth and coalescence (NGC) of micro-dimples [18–20]. The features showed on the surfaces are typical of a high toughness material. From the SEM fractographs of Fig. 2(a and b), it is evident that the inclusions contribute significantly to the fracture process. In these fractographs, arrows labeled 2 and 4 show some dimples holding inclusions of irregular and spherical form respectively. While the different events which conform the fracture process including the nucleation of a dimple and its subsequent growth to cause final coalescence are at times difficult to differentiate between, it is certain that inclusions are responsible for the initiation of a general crack in high toughness materials [21,22]. Other characteristic features of these fracture surfaces are the several regions of shear localization between voids, consisting of small dimples or void sheets nucleated at later stages of the plastic deformation, some of which are shown in regions 1 and 3. Empty shallow dimples as the one in region 5 are also visible on both fracture surfaces.

As in the previous fractographs, Fig. 2(c) shows a complex grid of fine voids or void sheets (region 6) around the big dimples. It was noted that for 0, 3 and 9 h of aging, the average dimple was roughly equiaxed. One of these regular dimples is shown at 7. While the fracture surfaces of the steel shown in Fig. 2(a–c) were Mode I dominated with limited evidence of localized shear, the surface corresponding to the 24 h of aging (Fig. 2(d)) shows that the fracture occurs by a localized mixed Mode I/II leading to a partially shear rupture of void coalescence mechanism. Two characteristic parabolic dimples commonly observed in this kind of mixed mode of fracture are shown in Fig. 2(d) in regions 9 and 10. Also, an inclusion associated to a parabolic dimple is observed in the same figure at 8. From a statistical point of view the impact behavior of the studied alloy is uniform for the range of aging times between 0 and 24 h, as can be seen in Table 2. Averaging over the entire range of data (0–24 h), the corresponding absorbed energy becomes

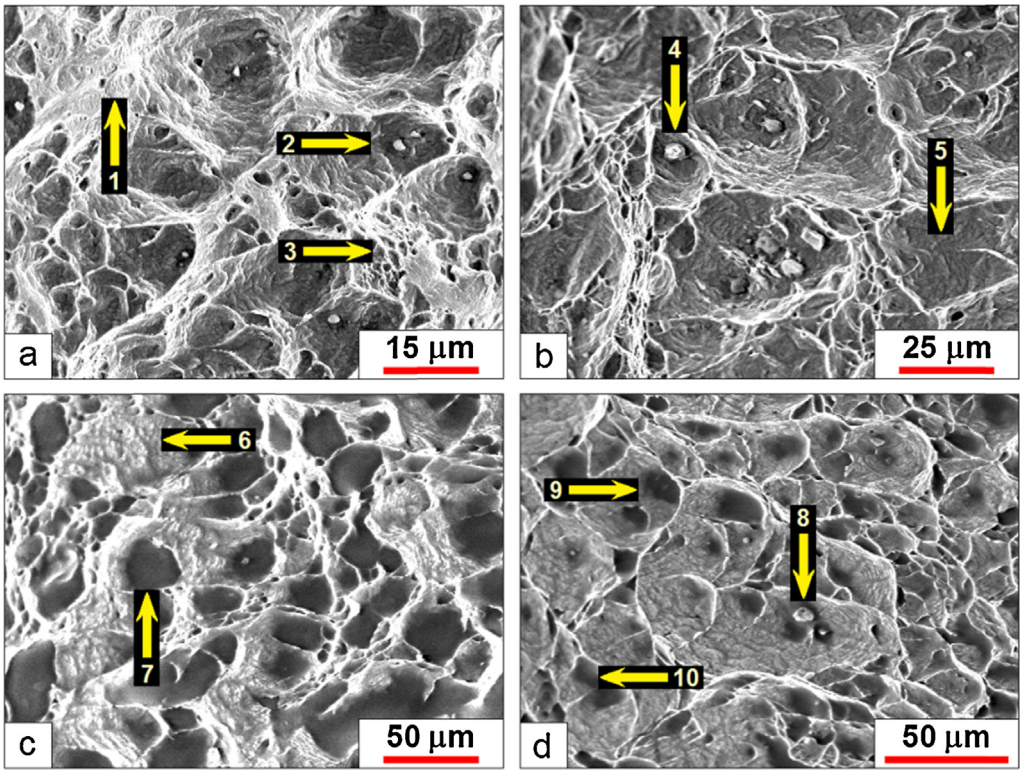

Fig. 2. SEM fractographs of the broken samples of SAF 2507 SDSS, aged at 475 °C for: (a) 0 h; (b) 3 h; (c) 9 h and (d) 24 h.

≈284 J (nearly the same average value corresponding to 9 h of aging).

3.1.2. Samples aged between 72 and 288 h

Fig. 3 shows the fractographs of the impact samples aged between 72 and 288 h. The fractograph depicted in Fig. 3(a) (72 h of aging) shows a void sheet in region B separating two dimpled zones in regions A and C. Shear rupture of void coalescence mechanism prevails in region A, whereas Mode I is predominant in region C. Typical equiaxed and parabolic dimples holding inclusions labeled 1 and 2 are seen in zones C and A respectively. With regard to the impact toughness, its value drops about 32% as compared to the material aged between 0 and 24 h. On the other hand, contrary to the previous fracture topographies, Fig. 3(b–d) (120, 192 and 288 h of aging) show fracture surfaces predominantly brittle with few areas of ordinary ductile fracture (as the void region shown in 5). For these brittle fracture surfaces it was noted the presence of many characteristic cleavage facets as can be seen in 4, 7, 8, 9, 10 and 11. An example of the low ductility of these brittle fracture surfaces is readily appreciated from the inclusion shown at 6, where the associated dimple has not been well developed. In despite of their brittle appearance, the fracture surfaces depicted in Fig. 3(b and c) are related to a relative high energy absorption values, as can be seen in Table 2. On the other hand, the SAF 2507 SDSS has an inherent high impact toughness, which can be explained in terms of the deformation of the austenite islands according to the rupture mechanism model developed by Verhaegue et al. [23] in an austenoferritic duplex steel. This rupture mechanism model involves an atypical fracture surface morphology which consists of an array of cleavage facets in the ferritic phase intercalated with deformation holes in the austenitic phase. Several holes of this type associated to the plastic deformation of the austenite and surrounded by many cleavage facets can be seen in 3 and 12 (Fig. 3(b and d) respectively). The lowest impact toughness (43 J) was reached after 288 h of aging (Fig. 3(d)).

Table 2
Impact energy data for different times of aging at 475 °C.

Time t (h)	0	3	9	24	72	120	192	288
Impact toughness, I (J)	300.00	300.00	296.31	296.18	198.31	146.19	109.81	69.14
	300.00	300.00	295.91	287.98	197.55	136.21	107.27	64.61
	300.00	298.50	282.69	272.21	214.93	124.00	101.42	41.70
	299.50	297.10	278.43	239.41	190.15	115.90	81.00	21.12
	299.10	295.81	269.91	173.17	169.66	112.00	80.40	19.88
$\bar{I} \pm \sigma$ (J)	299.72 ± 0.37	298.28 ± 1.64	284.65 ± 10.22	253.79 ± 44.75	194.12 ± 14.67	126.86 ± 12.73	95.98 ± 12.77	43.29 ± 20.81

3.2. Ferrite embrittlement and fracture topography

According to the above mentioned rupture mechanism model [23] although solution annealed and low-time aged duplex austenoferritic alloys usually fail in a ductile way in both austenitic and ferritic phases, for long enough time of aging, the material shows that cleavage cracks nucleate in the embrittled ferrite and do not propagate in a catastrophic way in the material, as the austenite remains ductile. Once nucleated, the propagation of a cleavage crack in ferrite is controlled by plasticity of the surrounding austenite.

For a brittle fracture surface in a duplex steel, the propagation of a crack nucleated in ferrite can be described in two steps. First: the crack is extended from the size of the nucleous up to the spacing between austenite islands, blunting in austenite where the crack tip lies at a ferrite/austenite interface. Second: the crack moves into the austenite, and its extension is controlled by the stretching of the austenite ligaments that have been passed round. Thus, the fracture surface consists of numerous cleavage facets in ferrite, surrounded by holes of different morphologies developed in the austenite phase, which can be seen in the fractographs of Fig. 3(b and d).

The embrittlement of the studied alloy is caused by the decomposition of the ferritic phase to chromium-rich phase, α' and iron-rich phase, α. The formation of α' occurs either through the mechanism of nucleation and growth or through spinodal decomposition [9,24]. Weng et al. [25] with the help of field-emission gun transmission electron microscopy (FEG-TEM), show that the fine scale isotropic spinodal decomposition of ferritic phase revealed chromium-rich bright image domains and iron-rich dark image domains, i.e. α' and α phases, separately. As only the ferritic phase is embrittled during aging treatment at 475 °C, the degradation in toughness directly depends on the state of the ferritic phase. From studies conducted by atom probe field ion microscope (APFIM) Miller and Bentley [26] suggested that the α' phase forms a complex interconnected network structure. This α' network grows as the aging time increases. As a consequence, the degree of embrittlement is enhanced.

3.3. General correlation between impact toughness and fractal dimension

For many authors the fractal dimension D can be regarded as a measure of the fracture toughness of materials [10–14,16,27–30]. Thus, fractal dimension can be used to monitor this property in an attempt to improve material strength or resistance to fracture. In spite of several controversies, there is a general agreement that the higher the toughness the rougher the fracture surface [10,13]. As the fractal dimension is considered a measure of roughness [31,32], the main topographical features on the fracture surface can be related to the values of D. Fig. 4 shows full logarithmic scale diagrams for the calculation of D. Since the fracture morphologies of the samples aged between 0 and 24 h are associated to the same mechanism of fracture, namely NGC of micro-dimples (Fig. 2), the corresponding

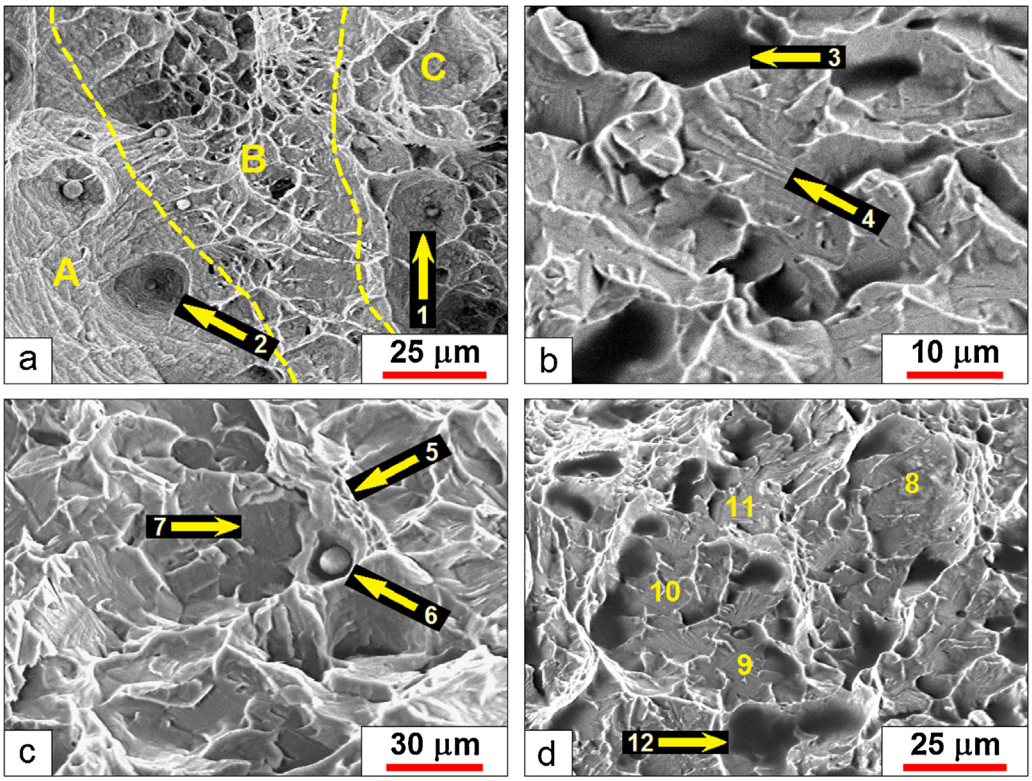

Fig. 3. SEM fractographs of the broken samples of SAF 2507 SDSS, aged at 475 °C for: (a) 72 h; (b) 120 h; (c) 192 h and (d) 288 h.

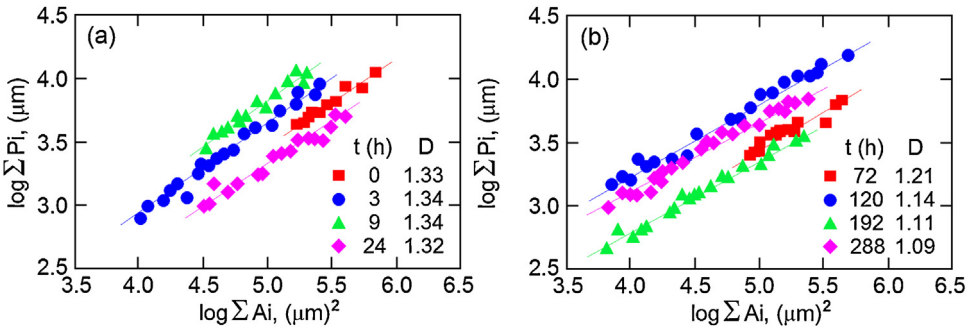

Fig. 4. Fractal perimeter–area relationship for the calculation of *D*. (a) Samples aged between 0 and 24 h. (b) Samples aged between 72 and 288 h.

values of *D* were very close, ranging between 1.32 and 1.34 (Fig. 4(a)). Apparently, the subtle differences between the geometry and the orientation of the dimples, are reflected in the fractal dimension values. For the high toughness fracture surfaces presented in Fig. 2 it is evident that the combination of a localized stress state and the presence of inclusions induces void initiation at the inclusion-ferrite and inclusion-austenite interfaces. These voids grow as the matrix undergoes plastic deformation while tearing around the inclusions. As a result of this process, deep holes develop generating an abrupt ridge-and-valley topography responsible for the relatively high fractal dimension values. When a partially shear rupture of void coalescence mechanism occurs (Fig. 2(d)), the edges of the dimples become roughly shallow and parabolic, generating a small reduction in *D*.

After 72 h of aging the fractal dimension of the corresponding impact sample shows a significant decrease, reaching a value of 1.21. This departure from the more or less uniform fractal behavior showed by the SDSS aged between 0 and 24 h, coincides with the already mentioned 32% decrease in toughness observed for the material aged for 72 h as compared to the material aged between 0 and 24 h. All the fracture surfaces obtained after impact tests of the samples aged during 72 h and represented in Fig. 3(a), show a mixture of Mode I and partially shear rupture of void coalescence mechanism, which accounts for the decrease in *D*. In light of these facts the fracture topography associated to the 72 h aging treatment can be regarded as a transitional one between low and high times of aging or alternatively, between ductile and brittle fracture behavior (Fig. 5).

From Fig. 3(b–d), it is apparent that the dominant fractographic feature for the samples aged between 120 and 288 h, is the cleavage facet, which results in a monotonically decrease in *D* as the time of aging increased. A lower *D* value is indicative of a decreased contribution of the cleavage facets to the roughness of these brittle fracture surfaces. Although the room temperature impact toughness of SAF 2507 SDSS decreased for increased times of aging between 120 and 288 h, it is considered that the absorbed energy in this range is still high enough as compared with the standards for most of the commercial metallic alloys.

The later particular behavior originates in the deflection of a cleavage crack nucleated in the embrittled ferrite when the crack tip lies at a ferrite/austenite interface. The plasticity of the austenite prevents an otherwise complete brittle behavior. In despite of this, the cleavage facets form a relatively low angles with the local mean plane of fracture, generating a lower surface relief and a lower fractal dimension. The impact toughness-fractal dimension relationship for the aged SAF 2507 SDSS is summarized in Fig. 5. In regard to this figure, several important comments are relevant: the data related with the aging treatments made between 0 and 24 h, which represent an statistically uniform behavior, have been averaged in a single datum, being 284 J the impact toughness and 0.33 the corresponding fractal dimensional increment. On the other hand, the data of the impact toughness for 288 h of aging, as can be seen in Table 2, show a high dispersion ($\sigma = \pm 20.81$ J) around a comparative low average impact toughness value of 43.29 J, so the datum for 288 h of aging was not considered for the statistical correlation developed between the impact toughness and D^*. The adjustment of the linear relation between *I* and D^* was made using a least-squares program, being the squared correlation coefficient for the rest of the data: $r^2 = 0.999$. Before describe the mathematical relation between *I and* D^* for SAF 2507 SDSS, it is pertinent to briefly discuss some previous important models, in order to sustain such a relation.

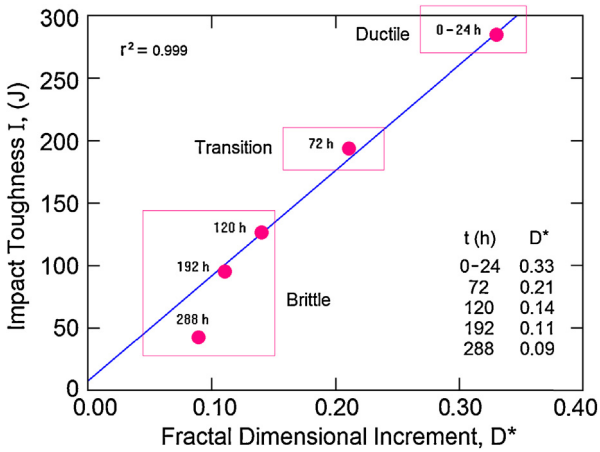

Fig. 5. The variation of the impact toughness at room temperature with fractal dimensional increment in SAF 2507 SDSS (the datum for 288 h was not considered for the statistical positive correlation between *I* and D^*).

3.3.1. Some previous relations between toughness and fractal dimension

Today a satisfactory explanation to distinguish between ductile and brittle fracture is not available. Williford [33] analyzed the collected data of positive and negative correlation between toughness and D and plotted an analogy to the dimension spectrum as a multifractal. Williford [33] established a positive relation between toughness and fractal dimension for brittle materials (ceramics), a negative relation for ductile materials (metallic alloys) and no correlation for composites materials. As the experimental results of fractal dimension and toughness were obtained by using different methods under different experimental conditions, some doubts about the soundness of the data could emerge. On the other hand, although Williford [33] as well as other authors [14,27,34] reported a negative correlation between fractal dimension and toughness for several metallic materials using the slit island method (SIM), it was demonstrated that this correlation was unrealistic [16] and explained as the result of using a relatively large ruler length η, which destroys the basis of self-similarity. Using the SIM a positive correlation between fractal dimension and toughness is obtained for metallic materials [35–37] when the length η of the ruler used to estimate the perimeter and the area of the metallic "islands", becomes smaller than a critical value [16]. A good example of this was presented in the work of Tsiung and Chou [37], who found that the fractal dimension increases with increasing impact toughness for ruler lengths of 0.666 μm and 0.2664 μm, but when a ruler length of 6.66 μm was used, a negative correlation was obtained. Tsiung and Chou [37] studied a high-strength low-alloy steel and the relation between the impact toughness and the fractal dimension, covered not just the ductile range but the brittle range too. We think that the correct choice of η using the SIM is still an unsolved problem. On the other hand, as the fracture phenomenon is very complex, and so many factors play important roles, it is not surprising that the correlation between fractal dimension and toughness adopts any sign for metallic materials, even more if we take into account that, unfortunately, there are strong variations in the fractal dimension measured in different studies depending of the method of measurement (Milman et al. [10]).

Nagahama [28] proposed a model which is based on the Griffith energy balance concept. He postulates an average size of void pits on the fracture surface ε, normalized by the average size of void pits on the fracture surface produced under the brittle–ductile transitional condition. The relation derived by Nagahama [28] has the form

$$\log K_C = A + \frac{1}{2}(2 - D) \log \varepsilon \tag{2}$$

where K_C is the fracture toughness, A is a constant, D is the fractal dimension and $(2 - D) \leq 0$. In the case of ductile fracture, since $\log \varepsilon > 0$, it will be observed a lower fracture toughness for a higher fractal dimension (Eq. (2) of the negative type). In the case of brittle fracture, since $\log \varepsilon < 0$, it will be observed a higher fracture toughness for a higher fractal dimension (Eq. (2) of the positive type). For the case of metallic materials Nagahama suggests [28] that the Eq. (2) is always of the same kind (negative one). We can conclude from this model that in the case of metallic materials, a dimple is the characteristic fracture feature (structure parameter) for both, ductile and brittle fracture. We think that in order to be a structure parameter for a specific fracture surface, the corresponding fracture feature must be the dominant one. It follows that if *dimples* are present in a *brittle* fracture, they cannot be the *characteristic* structure parameter.

Nagahama states [28] (after Lung [38]) that: "Brittle fractures would be formed by microvoids, irregular distribution of vacancy clusters, inclusions and microcracks, which govern the localization of small ductile deformations". From the point of view of the characteristic fracture feature of a brittle fracture surface in metallic alloys, this statement is not clear at all. In brittle fracture the voids are located in small zones of ductile nature, and, for this reason, the voids itself do not predominate because they are very low in number. On the contrary, microcracks (closely associated to cleavage facets and river patterns) should be the characteristic feature in brittle fracture surfaces.

Carney and Mecholsky [12] extended the model developed by Mecholsky et al. [31,39,40] initially proposed for ceramic materials, to the study of the relation between fracture toughness and fracture surface fractal dimension in a metallic alloy (4340 steel). This model has been the result of the linear characteristics of the experimental data, combined with the required dimensional adjustments. For 4340 steel they obtained a relation between K_{IC} and D^* of a negative nature, being the corresponding equation of the form

$$K_{IC} = K_o - AD^{*\,1/2} \tag{3}$$

where K_{IC} is the plane strain fracture toughness, D^* is the fractal dimensional increment $(0 \leq D^* \leq 1)$, $K_o = 250\,\text{MPa}\,\text{m}^{1/2}$ is a constant (maximum value of K_{IC} for $D^* = 0$), and $A = 402\,\text{MPa}\,\text{m}^{1/2}$ is a constant composed of $E(a_o)^{1/2}$, E = Young's modulus and a_o = a material dependent structure parameter. As $E \approx 200$ GPa, a_o becomes 4.0×10^{-6} m, a value of the order of the largest dimples observed on the fracture surfaces of the ductile samples of 4340 steel.

For SAF 2507 SDSS the relation between I and D^* was of a positive type. The corresponding analytical description was partially based on both, a model presented by Carney and Mecholsky [12] and several concepts developed by Mecholsky et al. [41].

3.3.2. Analytical relation between impact toughness and D^* for SAF 2507 SDSS

The adjustment of the linear relation between I and D^* was made on the basis of the four data points corresponding to: 0–24 h; 72 h; 120 h and 192 h. This relation is given by

$$I = I_o + AD^* \tag{4}$$

where $I_o = 7.52$ J is a constant (minimum value of I for $D^* = 0$) and $A = 849$ J is a constant composed of EV_c, E = Young's modulus and V_c = critical volume of material. Mecholsky et al. [41] describes a non-equilibrium fracture process for materials that fail in a brittle fashion (ceramics) which begins with separation of primary bonds at the atomic

level, creating a free volume as a result of discrete geometric reconfigurations along the tip of the crack front. In despite of the obvious differences between ceramic and metallic materials an analogy can be established with the suggestions of Mecholsky et al. [41], since V_c (which is not considered here a free volume) can be somewhat related with the process which leads to the formation of a plastic zone, normally developed along the tip of the crack front. V_c can be calculated using the value of the constant A and the value of E for SAF 2507 SDSS [42], which is about 200 GPa. Since $A = 849\,\text{Nm} = 200 \times 10^9\,\text{N/m}^2 \times V_c$, it follows that $V_c = 4.25 \times 10^{-9}\,\text{m}^3$, or $4.25\,\text{mm}^3$.

For the sake of simplicity, we can assume a cylindrical critical volume of length ℓ, which diameter can be taken as a critical length a_c. As V_c can be associated to the total length of the crack front, the magnitude of ℓ is considered, as a first approximation, of the same order of the crack front originated from the notch of a Charpy impact sample, i.e. $\ell \approx 10\,\text{mm}$. Then, the critical diameter can be written as $a_c = 2[V_c/\ell\pi]^{1/2} \approx 0.736 \times 10^{-3}\,\text{m} = 736\,\mu\text{m}$. Fig. 6a shows the relation between the crack front and the critical volume of diameter a_c. Although there is no intention here to further develop this concept, it is pertinent to indicate that the critical volume resembles in some way the classical plastic zone, which spreads along the crack front across the thickness of the samples used in linear elastic fracture mechanics (LEFM), so the critical volume is as large as the corresponding crack front. As has been quoted by Carney and Mecholsky [12], Ritchie et al. [43] proposed that a critical length (microstructurally significant distance) of 100–300 μm could be related with the unstable crack propagation in metallic alloys depending on several experimental variables. If we assume that V_c is related with the unstable crack propagation, its critical diameter a_c could be considered the corresponding critical length. Then, for SAF 2507 SDSS, the value of the critical length ($a_c = 736\,\mu\text{m}$) is about 2.5 times higher than the highest value suggested by Ritchie et al. [43], which can be partially justified based on the inherent high toughness of this alloy.

On the other hand, Carney and Mecholsky [12] suggest that a critical length could be developed after several sub-units of length a_o (a material dependent structure parameter), join together over the microstructurally significant distance, and showed that for 4340 steel the structural parameter a_o is associated with the largest dimples on the fracture surface (4.0×10^{-6} m). Again, establishing an analogy with the work of Mecholsky et al. [41], we can say that the parameter a_o could be a measure of the structure upon which the critical volume V_c is created. As a_c is composed of several sub-units of length a_o, we can write: $a_c = \lambda a_o$, where λ is the number of sub-units. Fig. 6(b) shows a schematic of the formation of a critical volume of material at the crack tip of a growing crack. For this critical volume $a_c = \lambda a_o$.

In general terms, for the same material, if the fracture surface is ductile, the damage is in the form of plastic deformation (dimples) and if the fracture surface is brittle, the damage is in the form of microcracking (cleavage facets). We think that no matter the nature of the fracture surface, the structural parameter for the same material is of the same length, but associated to a different surface feature. A careful examination of Figs. 2 and 3 reveals that for both, ductile and brittle fracture surfaces, the largest dominant fracture features (dimples and cleavage facets respectively) have approximately the same size, i.e. about 30×10^{-6} m, which corresponds to the size of a "generic" structure parameter a_o. The constant A can be rewritten as

$$A = EV_c = E\left[\pi\left(\frac{a_c}{2}\right)^2 \ell\right] = E\left[\pi\left(\frac{\lambda a_o}{2}\right)^2 \ell\right] = \frac{\pi}{4}\ell E(\lambda a_o)^2 \tag{5}$$

where $(\pi/4)\ell$ is a constant associated to the morphology of the critical volume V_c, and the value of λ is $\approx$24.5 (736 μm/30 μm). Then, the relation between I and D^* becomes

$$I = I_o + \frac{\pi}{4}\ell E(\lambda a_o)^2 D^* \tag{6}$$

Hilders et al. [8,44] studied the fractal characterization of fracture surfaces of an aged SAF 2205 duplex stainless steel broken in tension at 25 °C and obtained a similar trend between fractal dimension and ductility;the higher

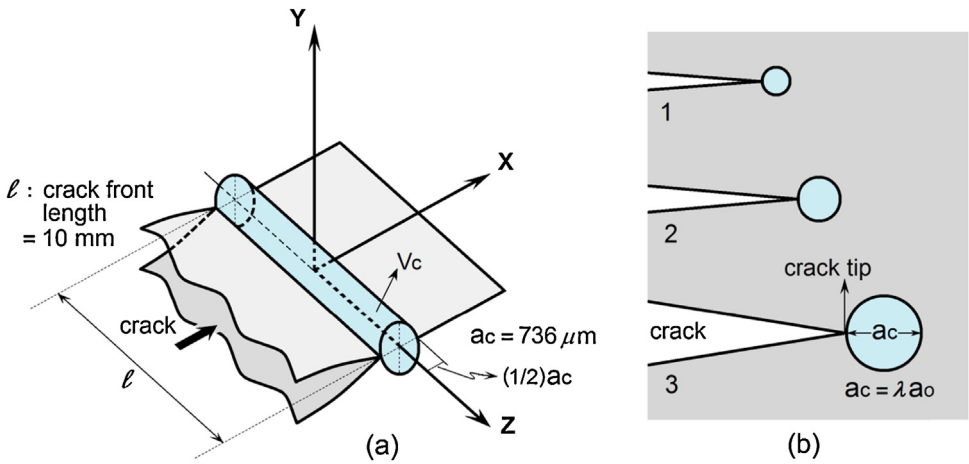

Fig. 6. (a) Relation between the critical volume V_c of diameter a_c, and the crack front, for a Charpy impact sample. (b) Critical volume developed ahead of the crack tip of a growing crack.

the time of aging, the lower the ductility and the fractal dimension. In addition, as expected, it was observed a concomitant increase of the tensile strength. Then, it could be possible to use the fractal dimension as a characterization parameter in fracture morphology–mechanical properties studies, in several stainless steels of the duplex family.

Several conjectures made in this work are inconclusive and yet to be substantiated, so further research is needed in order to clarify the fractal characteristics of the SAF 2507 SDSS, and other alloys of this family. Understanding of the fractal properties of the fracture surface and the toughness of metallic materials has proven to be elusive. Despite of many investigations, there exists no general acceptable analytical description of toughness–fractal dimension relationship, partly to the rather complex nature of the fracture phenomenon. We think that there is still much research to be done in this field, even in the traditional materials which have been used for many years.

4. Conclusions

In this experimental study on establishing the influence of aging treatments at 475 °C on the fractal dimension of the fracture surfaces and impact toughness at room temperature of SAF 2507 SD SS, the following observations are made:

(1). For the impact samples aged between 0 and 24 h ductile fracture occurred by NGC of micro-dimples, with the large dimples initiating at inclusion particles. The impact behavior was uniform for this range of aging time, being 284 J the average absorbed energy.

(2). The impact samples aged for 72 h show a mixture of shear and normal rupture of void coalescence mechanism, with parabolic and equiaxed dimples holding inclusions. The fracture topography associated to this time of aging can be regarded as a transitional one between ductile and brittle fracture. An impact toughness of 194 J was observed for this condition.

(3). For the impact samples aged between 120 and 288 h, the dominant fractographic feature is the cleavage facet in the ferritic phase. Although the general behavior of these samples can be regarded as brittle, it is considered that the absorbed energy in this range is relatively high (127-43 J).

(4). For the impact samples aged between 120 and 288 h, the propagation of a cleavage crack in ferrite is controlled by the plasticity of the surrounding austenite. As a result, an atypical fracture surface morphology which consists of an array of cleavage facets in the ferritic phase intercalated with deformation holes in the austenitic phase is developed.

(5). As the time of aging increases from 0 to 288 h a monotonically decrease in D^* was observed and the impact fracture surfaces changed from ductile to brittle appearance.

(6). Partially based on several previous concepts and relationships well established for brittle materials [12,31,39–41], a direct linear correlation between impact toughness and fractal dimensional increment has been developed. The concept of critical volume of material is proposed and tentatively related with the unstable crack propagation event, through both, the so called critical length (microstructurally significant distance) and the size of the largest micro-dimple and cleavage facet (structural parameter) developed in ductile and brittle fracture respectively.

Conflict of interest

The authors have no conflict of interest to declare.

Acknowledgement

Research supported by the Scientific and Humanistic Development Council of the Central University of Venezuela and the Venezuelan College of Engineering.

References

[1] Pardal JM, Tavares SSM, Fonseca MPC, Sousa JA, Vieira LM, Abreu HFG. Deleterious phases precipitation on superduplex stainless steel UNS S32750: characterization by light optical and scanning electron microscopy. Mater Res 2010;13:401–7.
[2] Lee JS, Jeon SH, Park YS. Effects of solution annealing temperature on the galvanic corrosion behavior of the super duplex stainless steels. J Mater Eng Perform 2013;22:557–62.
[3] Lo KH, Shek CH, Lai JKL. Recent developments in stainless steels. Mater Sci Eng R Rep 2009;65:39–104.
[4] Tehovnik F, Arzenšek B, Arh B, Skobir D, Pirnar B, Žužek B. Microstructure evolution in SAF 2507 super duplex stainless steel. Mater Technol 2012;45:339–45.
[5] Nilsson JO, Wilson A. Influence of isothermal phase transformations on toughness and pitting corrosion of super duplex stainless steel SAF 2507. Mater Sci Technol 1993;9:545–54.
[6] Dobranszky J, Szabo PJ. EDS analysis of intermetallic precipitation in thermally aged SAF 2507 type super duplex stainless steel. Mater Sci Forum 2003;414–415:189–94.
[7] Hattestrand M, Larsson P, Chai G, Nilsson JO, Odqvist J. Study of decomposition of ferrite in a duplex stainless steel cold worked and aged at 450–500 °C. Mater Sci Eng A 2009;499:489–92.
[8] Hilders OA, Sáenz L, Ramos M, Peña ND. Effect of 475 °C embrittlement on fractal behavior and tensile properties of a duplex stainless steel. J Mater Eng Perform 1999;8:87–90.
[9] Sahu JK, Krupp U, Ghosha RN, Christ HJ. Effect of 475 °C embrittlement on the mechanical properties of duplex stainless steel. Mater Sci Eng A 2009;508:1–14.
[10] Milman VY, Stelmashenko NA, Blumenfeld R. Fracture surfaces: a critical review of fractal studies and a novel morphological analysis of scanning tunneling microscopy measurements. Prog Mater Sci 1994;38:425–74.
[11] Hilders OA, Pilo D. On the development of a relation between fractal dimension and impact toughness. Mater Charact 1997;38:121–7.
[12] Carney LR, Mecholsky Jr JJ. Relationship between fracture toughness and fracture surface fractal dimension in AISI 4340 steel. Mater Sci Appl 2013;4:258–67.
[13] Hilders OA, Ramos M, Peña ND, Sáenz L. Fractal geometry of fracture surfaces of a duplex stainless steel. J Mater Sci 2006;41:5739–42.
[14] Mu ZQ, Lung CW. Studies on the fractal dimension and fracture toughness of steel. J Phys D Appl Phys 1988;21:848–50.
[15] Lung CW, March NH. Mechanical properties of metals, atomistic and fractal continuum approaches. 1st ed. Singapore: World Scientific Publishing Co.; 1999.
[16] Lung CW, Mu ZQ. Fractal dimension measured with perimeter-area relation and toughness of materials. Phys Rev B 1988;38:781–4.
[17] Hilders OA. Strength ductility and fractal characteristics of an Al–0.57Si–2.03Ge alloy. In: Sato T, Kumai S, Kobayashi T, Murakami Y, editors. Aluminum alloys their physical and mechanical properties. Tokyo: The Japan Institute of Light Metals; 1998. p. 955–60.
[18] Tvergaard V, Hutchinson JW. Two mechanisms of ductile fracture: void by void growth versus multiple void interaction. Int J Solids Struct 2002;39:3581–97.

[19] Benzerga AA. Micromechanics of coalescence in ductile fracture. J Mech Phys Solids 2002;50:1331–62.
[20] Ma D, Chen D, Wu S, Wang H, Cai C, Deng G. Dynamic experimental verification of void coalescence criteria. Mater Sci Eng A 2012;533:96–106.
[21] Garrison Jr WM, Wojcieszynski AL. A discussion of the effect of inclusion volume fraction on the toughness of steel. Mater Sci Eng A 2007;464:321–9.
[22] Garrison Jr WM, Wojcieszynski AL. A discussion of the spacing of inclusions in the volume and of the spacing of inclusions nucleated voids on fracture surfaces of steels. Mater Sci Eng A 2009;505:52–61.
[23] Verhaegue B, Louchet F, Bréchet Y, Massoud JP. Damage and rupture mechanisms in an austenoferritic duplex steel. Acta Mater 1997;5:1811–9.
[24] Tavares SSM, de Noronha RF, da Silva MR, Neto JM, Pairis S. 475 °C Embrittlement in a duplex stainless steel UNS S31803. Mater Res 2001;4:237–40.
[25] Weng KL, Chen HR, Yang JR. The low-temperature aging embrittlement in a 2205 duplex stainless steel. Mater Sci Eng A 2004;379:119–32.
[26] Miller MK, Bentley J. APFIM and AEM investigation of CF8 and CF8M primary coolant pipe steels. Mater Sci Technol 1990;6:285–92.
[27] Mandelbrot BB, Passoja DE, Paullay AJ. Fractal character of fracture surfaces of metals. Nature 1984;308:721–2.
[28] Nagahama H. A fractal criterion for ductile and brittle fracture. J Appl Phys 1994;75:3220–2.
[29] Chang Q, Chen D, Ru H, Yue X, Yu L, Zhang C. Three-dimensional fractal analysis of fracture surfaces in titanium-iron particulate reinforced hydroxyapatite composites: relationship between fracture toughness and fractal dimension. Journal of Materials Science 2011;46:6118–23.
[30] Pramanik B, Tadepalli T, Mantena PR. Surface fractal analysis for estimating the fracture energy absorption of nanoparticle reinforced composites. Materials 2012;5:922–36.
[31] Mecholsky Jr JJ, Passoja DE, Feinberg-Ringel KS. Quantitative analysis of brittle fracture surfaces using fractal geometry. J Am Ceram Soc 1989;72:60–5.
[32] Balankin AS. Physics of fracture and mechanics of self-affine cracks. Eng Fract Mech 1997;57:135–203.
[33] Williford RE. Multifractal fracture. Scr Metall 1988;22:1749–54.
[34] Su H, Zhang Y, Yan Z. Fractal analysis of microstructures and properties in ferrite-martensite steels. Scr Metall Mater 1991;25:651–4.
[35] Wang ZG, Chen DL, Jiang XX, Ai SH, Shih CH. Relationship between fractal dimension and fatigue threshold value in dual-phase steels. Scr Metall 1988;22:827–32.
[36] Ray KK, Mandal G. Study of correlation between fractal dimension and impact energy in a high strength low alloy steel. Acta Metall Mater 1992;40:463–9.
[37] Tsiung JC, Chou YT. Fractal characterization of the fracture surface of a high strength low-alloy steel. J Mater Sci 1998;33:2949–53.
[38] Lung CW. Fractals and the fracture of cracked metals. In: Pietronero L, Tosatti E, editors. Fractals in physics. Amsterdam: Elsevier Science; 1986. p. 189–92.
[39] Mecholsky Jr JJ, Freiman SW. Relationship between fractal geometry and fractography. J Am Ceram Soc 1991;74:3136–8.
[40] Mecholsky Jr JJ. Quantitative fractography: an assessment. In: Varner JR, Frechette VD, editors. Ceramics transactions: fractography of glasses and ceramics II. Westerville: American Ceramic Society; 1991. p. 413–51.
[41] Mecholsky Jr JJ, West JK, Passoja DE. Fractal dimension as a characterization of free volume created during fracture in brittle materials. Philos Mag A 2002;82:3163–76.
[42] Ponthot JP, Guo WC, Rauchs G, Zhang WH. Influence of friction on imperfect conical indentation for elastoplastic material. Tribology 2009;3:151–7.
[43] Ritchie RO, Server WL, Wullaert RA. Critical fracture stress and fracture strain models for the prediction of lower and upper shelf toughness in nuclear pressure vessel steels. Metall Trans A 1979;10:1557–70.
[44] Hilders OA, Sáenz L, Peña N, Ramos M, Quintero A, Caballero R, et al. Fractal characterization of the fractured surface of a duplex stainless steel and its relation with strength and ductility. In: Bailey GW, McKernan S, Price RL, Walck SD, Charest PM, Gauvin R, editors. Microscopy and microanalysis 2000. Philadelphia: Springer; 2000. p. 766–7.